# Effects of Gly residue and Cholesterol on the GXXXG-Mediated Parallel Association of Transmembrane Helices: A Single-Pair FRET Study

Yoshiaki Yano,[a] Takayuki Morise,[b] and Katsumi Matsuzaki*[b]

[a] Prof. Y. Yano

School of Pharmacy and Pharmaceutical Sciences, Mukogawa Woman's University,

Nishinomiya 663-8179, Japan

[b] T. Morise, Prof. K. Matsuzaki

Graduate School of Pharmaceutical Sciences, Kyoto University, Kyoto 606-8501, Japan

E-mail: mkatsumi@pharm.kyoto-u.ac.jp

## Abstract

Small residue-mediated interhelical packing is ubiquitous in helical membrane proteins: however, the lipid dependence of its stability remains unclear. We previously demonstrated that the introduction of a GXXXG sequence in the middle of *de novo*-designed $(AALALAA)_3$ helices (AALALAA AGLALGA AALALAA) facilitated their dimerization, which was abolished by cholesterol. Here single-pair FRET measurements revealed that a longer GXXXGXXXG segment (AALALAA A GLALGA AAGALAA) promoted helix dimerization in POPC/cholesterol bilayers, but not without cholesterol. The predicted dimer structures and degrees of helix packing suggested that helix dimers with small (~10°) and large (~55°) crossing angles were only stabilized in POPC and POPC/cholesterol membranes, respectively. A steric hindrance in the dimer interface and the large flexibility of helices prevented the formation of stable dimers. Therefore, amino acid sequences and lipid compositions distinctively constrain stable dimer structures in membranes.

# Introduction

The amino acid sequences of transmembrane (TM) helices in integral membrane proteins dictate not only TM localization by their hydrophobicity but also possible helix interfaces that mediate helix–helix associations for the formation of protein tertiary structures and protein oligomers.[1] Small residues (particularly glycine pair(s)) in the TM region uniquely stabilize the self-association of TM helices in membrane environments with a defined range of the crossing angles (the angle between the axes of the helices).[2] The strength of these interactions was previously proposed to be context-dependent (amino acid sequences and lipid compositions).[3] It is well-known that steric hindrance around the Gly-containing surface affects the degree of helix packing.[2a] However, the mechanism of interplay between amino acid sequences and lipid compositions remains unclear. Membrane cholesterol is an important regulator of protein activities through direct and indirect mechanisms.[4] Cholesterol directly binds to cholesterol-binding pockets or the sequence motifs of target proteins in order to regulate protein conformations.[5] Alternatively, membrane cholesterol may change membrane properties to indirectly induce structural rearrangements or stabilize

helices.[6] However, the mechanisms by which helix–helix associations are regulated by the indirect mechanism remain unknown.

The activities of membrane proteins are often affected by the lipid composition as revealed by experiments using liposomes that reconstitute purified membrane proteins.[7] However, real proteins and natural TM helices from them often have multiple and complex interhelical interactions. A reasonable way to avoid such complexity in measurements of the interactions is the use of model TM helices with simple and designed amino acid sequences. Investigation of self-association of such model TM helices is a powerful approach to reveal the effects of side chain interactions and lipid environments on TM helix–helix interactions.[8] Although the TM helix interactions have been considered as principal interactions that determine the folding of TM proteins, the loop regions between transmembrane helices can also have an impact on the folding of TM proteins,[1a] the latter is out of scope of the model TM helix approach. To elucidate the indirect effects of lipid compositions on interactions between TM helices, we examined the self-associations of model TM helical peptides with a *de novo*-designed sequence ($(AALALAA)_3$, designated as Host in Table 1) and

related peptides.[9] The Host helix, which is devoid of sequence motifs for self-association, is useful for investigating the effects of amino acid substitutions and lipid environments on TM helix–helix interactions. Such information not only provides fundamentals to understanding the stabilities of TM proteins but is also valuable for *de novo* protein design,[10] and benchmark of computer simulation studies.[11] We found that membrane cholesterol significantly stabilized host dimers[9c] and also that 3- and 4-helix bundles comprised host helices.[9e]

In the present study, we investigated the effects of sequences in the vicinity of guest GXXXG motifs (Table 1) on the parallel self-associations of TM helices in the absence and presence of cholesterol. Helices were synthesized as disulfide-bridged parallel dimers labeled with a donor (Cy3B) and acceptor (Cy5) of fluorescence resonance energy transfer (FRET) (Supporting Information, Figures S1 and S2). They were then incorporated into 1-palmitoyl-2-oleoyl-*sn*-glycero-3-phosphatidylcholine (POPC) or POPC/cholesterol liposomes under dilute conditions (1 dimer per ~10 liposomes) and treated with disulfide-reducing β-mercaptoethanol. The self-association dynamics of two helix monomers were monitored in real time by single-pair FRET

(Figure 1).[9b] The purities of the synthesized disulfide-bridged peptides (labeled with Cy3B and Cy5) were moderate (>88%, HPLC, see also Supporting Information, Figures S1 and S2), although the major impurities were Cy3B–Cy3B and Cy5–Cy5 homodimers, the presence of which does not interfere the single-pair FRET analysis. To obtain structural information on the helix dimer, we performed Fourier transform infrared-polarized attenuated total reflection (FTIR-PATR) measurements using oriented films of lipids/peptides prepared on a germanium plate. We also discuss possible helix–helix dimer interfaces and the crossing angles based on the prediction by a computation program that predicts the stable packing interface from the amino acid sequences of helices (PREDDIMER).[12] This program generates two ideal α-helix structures having surface properties of given TM sequences, searches dimer structures with high surface complementarity by rotating the surfaces (evaluated as packing score $F_{scor}$), and then reconstitutes the 3D conformation (the rotation and crossing angles of the helices) of the putative dimer.

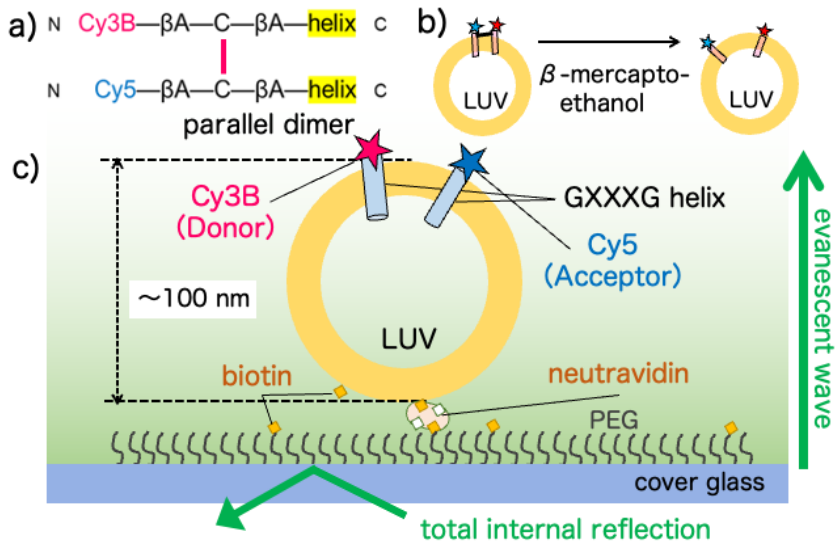


**Figure 1**

Single–pair FRET measurements. (a) Design of the parallel disulfide dimer. FRET donor (Cy3B) and acceptor (Cy5) fluorophores were labeled at the N terminus of the helix via β-alanine (βA) linkers. The purity and molecular weight of the synthesized peptides were examined by HPLC (Supporting Information, Figure S1) and mass spectroscopy (Supporting Information, Figure S2), respectively. (b) Control of insertion topology. After being incorporated into large unilamellar vesicles (LUVs) at a ratio of one dimer per ~10 vesicles, the helix dimer was reduced with mercaptoethanol to obtain two helices with a parallel insertion topology. (c) Schematic illustration of a surface-attached vesicle for single-pair FRET imaging by total internal reflection microscopy.

## Results and Discussion

We previously demonstrated that the introduction of a GXXXG sequence in the middle of the helix (AALALAA AGLALGA AALALAA, GXXXG1 in Table 1) facilitated dimerization in POPC ($\Delta G$ = –21.4 kJ mol$^{-1}$ at 25°C), which was abolished by cholesterol (see also Figure 2).[9b] Predictions of the dimer interface (Figure 3a) and Fourier transform infrared-polarized attenuated total reflection (FTIR-PATR) measurements (Table 2) revealed that the GXXXG1 dimer had a small crossing angle (~10°). This contrasts with a large crossing angle (50–60°) of the host dimer (hourglass-shaped or X-shaped dimer) stabilized in POPC/cholesterol membranes.[9b] Thus, only two Ala-to-Gly substitutions at positions 9 and 13 significantly altered stable dimer structures. The Gly surfaces with higher polarity preferentially pack with each other to avoid lipid exposure. The packing can also be stabilized by active forces such as polar and van der Waals interactions.[9b] On the other hand, the X-shaped dimers of GXXXG1 were destabilized even in the presence of cholesterol. This is at least in part because the introduction of Gly residues enhanced the flexibility of the main chain.[9b] Another cause of this destabilization is a steric hindrance in the X-shaped GXXXG1

dimer (see below). The absence of self-association of GXXXG1 in cholesterol-containing membranes also indicates that the dimer with a small crossing angle is not stable in the membranes. The incorporation of cholesterol decreases lateral pressures around the headgroup whereas increases the pressures near the center of the bilayer (see below for the detailed explanations for the lateral pressure profile). Such inhomogeneous change in the pressure profile was expected to be the reason why the dimer with a small crossing angle was destabilized in the presence of cholesterol.

GXXXG2 had an extended small-residue motif (GXXXGXXXG, L17G variant of GXXXG1, Table 1). Note that positions 5 and 17 are positioned along the interaction interface in the X-shaped dimer, whereas they are adjacent to the interaction surface in the dimer with a narrower shape (Supporting Information, Figure S3). If side chains of these positions are bulky in the X-shaped dimer, they can sterically interfere with each other (Supporting Information, Figure S3). Therefore, the L17G substitution was expected to reduce steric hindrance for the formation of an X-shaped dimer (Figure 3c). In contrast to GXXXG1, GXXXG2 self-associated in POPC/cholesterol (7/3) membranes (Figure 2). An analysis of the FRET trajectory estimated a $\Delta G$ value of –

22.3 kJ $mol^{-1}$ at 25°C. In contrast, FRET was not observed without cholesterol (Figure 2). Therefore, a change of only a single amino acid (L17G) between GXXXG1 and GXXXG2 completely reversed the cholesterol dependence of helix dimerization. FTIR-PATR spectra confirmed that GXXXG2 helices assumed helical structures (Supporting Information, Figure S4).

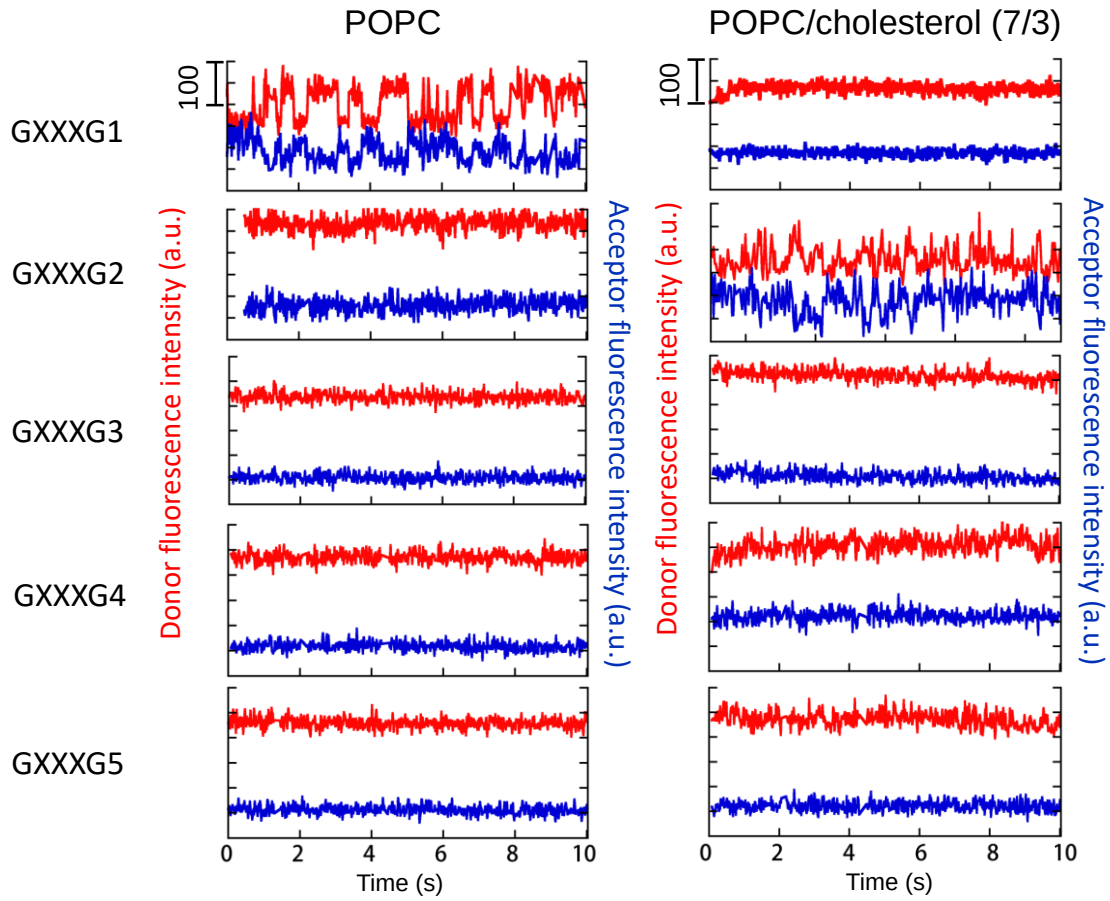


**Figure 2**

Representative time-courses of fluorescence intensities for Cy3B (red) and Cy5 (blue) under the excitation of Cy3B for GXXXG helices in POPC (left) and POPC/cholesterol (7/3) (right) at 25°C. The data for GXXXG1 were cited from a previous study.[7b] The number of analyzed vesicles for each condition was larger than 10. Regarding GXXXG2 in POPC/cholesterol, 11 vesicles were analyzed to estimate the association free energy (–22.3 kJ $mol^{-1}$).

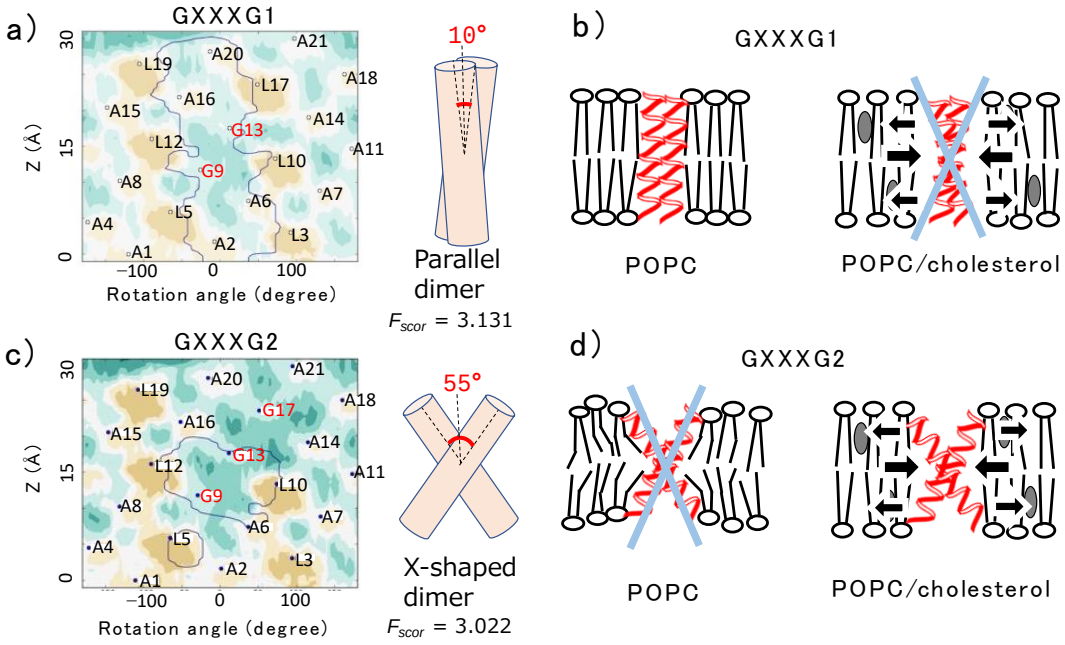


**Figure 3**

Relationship between the stable dimer structure and membrane composition. (a,c) The helix interaction interface of best-scoring dimers by PREDDIMER for GXXXG1 (a) and GXXXG2 (c). Horizontal and vertical axes indicate the helix rotation angle and distance along the helix (0 Å at the N terminus of the helix), respectively. Green and sand colors indicate low and high hydrophobicity regions, respectively, on the surface. The association interface region was surrounded by blue lines. The right image shows the shape of the dimers. (b, d) Combination of a stable dimer structure and membrane properties for GXXXG1 (b) and GXXXG2 (d).

Moreover, as evaluated from the dichroic ratio determined by the FTIR-PATR measurements, the GXXXG2 dimer was estimated to have a helix crossing angle of 52° in POPC/cholesterol (7/3) membranes (Table 2). This suggests the formation of a dimer with tilted helices.

To obtain further insights into the structure of the GXXXG2 dimer, we used the PREDDIMER computation program that predicts the stable packing interface from the amino acid sequences of helices.[12b] The best-scoring dimer structure for GXXXG2 had a large crossing angle (55°) (Figure 3c), which was close to the value estimated from the FTIR-PATR measurements (52°). These results suggested the formation of a stable X-shaped dimer for GXXXG2 in cholesterol-containing membranes (Figure 3d). This dimer is not stable in POPC due to the perturbation of lipid packing, and is stabilized in a cholesterol-containing membrane, in which the higher lateral pressure in the hydrocarbon core is partially released by the dimer. The smaller headgroup of cholesterol relative to the hydrophobic part significantly affects the lateral pressure profile (function of depth) of the lipid bilayers.[6c, 13] Lateral pressure is a global force

to balance the bilayer supramolecular structure, originating from entropic forces to satisfy hydrophobic interactions among nonpolar hydrocarbon chains and hydrophilic–hydrophobic size parameter of the component lipids. An interfacial tension (attracting force) at the water–membrane interface to minimize water–hydrocarbon chain contacts serve as a predominant negative lateral pressure at the interface position. To maintain a planner bilayer structure, this surface tension at the hydrophilic–hydrophobic interface is compensated for by repulsive forces (positive lateral pressures) at the headgroup and hydrophobic regions (in other words, the numerical integral of the lateral pressure across the bilayer should be zero). The repulsions that compensate for the interfacial tension include both electrostatic (in the headgroup region) and Pauli repulsions (in the headgroup and hydrophobic regions). Statistical thermodynamic calculations reported by Cantor suggest that incorporation of cholesterol into a C16:0 PC bilayer decreases pressures around the headgroup (0–7 Å from the interface) whereas increases pressures near the center of the bilayer (8–12 Å from the interface).[14] According to the change in the attraction–repulsion balance, the incorporation of cholesterol potentially increases and decreases the cross-sectional area of transmembrane proteins at the interface and

center of the membranes, respectively, to compensate for the cholesterol-induced stress by structural change of the protein. Such profile changes can stabilize the X-shaped transmembrane protein structure. Significant dimerization was only observed in the presence of cholesterol because an X-shaped dimer partially released higher lateral pressure in the hydrocarbon core induced by cholesterol;[9c] however, it appeared to disturb lipid packing in pure POPC membranes (Figure 3d). G17 in GXXXG2 should not interfere with the formation of the compact dimer by the steric hindrance of the side chain. However, PREDDIMER predicted a low packing score for such GXXXG2 compact dimer (crossing angle of 15°, $F_{scor}$ = 1.685, data not shown), implying that L17 of GXXXG1 positively contributes packing in the compact dimer. On the other hand, GXXXG1 can form a stable dimer with a small crossing angle (Figure 3b). Although this dimer is stable in POPC, it is destabilized in a cholesterol-containing membrane due to the inhomogeneous change in the lateral pressure profile (see above). An X-shaped dimer was not stable for GXXXG1 because of the steric hindrance of Leu17, which is consistent with the result showing that GXXXG1 formed a parallel dimer with a small crossing angle in POPC only (Figure 3b). The degree of FRET from the fluorescent

sterol, dehydroergosterol to NBD-GXXXG2 suggested the lack of a selective association (Supporting Information, Figure S5), supporting the model in which cholesterol indirectly promoted the self-association of GXXXG2.

GXXXG3 had a GXXGXXXGXXG motif (A6G and A16G substitutions relative to GXXXG1), and these four Gly residues were positioned on one interface of the helix (Supporting Information, Figure S6a). Due to the glycine cluster, GXXXG3 was expected to form a stable dimer with a small crossing angle. In practice, PREDDIMER predicted a parallel dimer structure with a high packing score. However, we did not observe any helix associations for GXXXG3 in POPC or POPC/cholesterol membranes (Figure 2). This discrepancy between the prediction and experiment was attributed to the higher flexibility of the helical secondary structure for GXXXG3 because of an increase in the number of Gly residues,[9b, 11b] which may abolish stable helix–helix associations. Consistently, the halfwidth of the amide I' band for GXXXG3 ($19.3 \pm 0.8$ cm$^{-1}$) was slightly larger than that for GXXXG2 ($17.7 \pm 0.4$ cm$^{-1}$) ($p$ = 0.07, two-tailed $t$-test) in POPC membranes (Supporting Information, Figure S7). Furthermore, the less reproducibility of the wavenumber of maximal intensity for

GXXXG3 supports the instability of its helical structure (Supporting Information, Figure S7). Since the prediction with PREDDIMER assumed the formation of ideal helical structures, it did not consider backbone flexibility. The role of Gly on disturbance of TM helices was controversial until recently and was systematically investigated using model TM helices by Langosch and colleagues.[15] They pointed out that the impact of Gly in TM helix flexibility might be obscured by stabilizing helix–helix packing, consistent with our observations.

We also examined the self-associations of GXXXG4 and GXXXG5 helices to confirm the effects of steric hindrance and the position of the GXXXG motif, respectively (Table 1). GXXXG4 was intended as a negative control of GXXXG1. In GXXXG4, an exchange of the residues of GXXXG1 at positions 5–6 and 16–17 resulted in the steric hindrance of side chains (leucine residues) in the interaction interface (Supporting Information, Figure S6b); therefore, poor interhelical packing was expected. Helix associations were not observed in POPC or POPC/cholesterol membranes (Figure 2). Furthermore, GXXXG5 was examined to clarify the effect of the position of the GXXXG motif. When the GXXXG motif was moved to the N

terminus (GXXXG5), the helix association was abolished again (Figure 2), which is consistent with the lower packing score (Figure 2, Supporting Information, Figure S6c). This demonstrates the importance of the central location of the GXXXG motif for helix self-association. It is not clear if the absence of N terminus Gly residues is important for the self-associations because the parallel self-associations of Host helices are too weak to be detected by sp-FRET measurements.[9b] The importance of the center position of the GXXXG motif was previously demonstrated using the TM sequences of glycophorin A and the bacteriophage M13 coat protein.[16]

## Conclusion

Our approach using model TM helices (GXXXG1–GXXXG5) revealed that a small number of amino acid substitutions resulted in dramatic changes in the cholesterol dependence of the GXXXG-mediated parallel helix associations. Although well-packed dimer structures can be considerably predicted from the amino acid sequence, our results revealed complex effects of cholesterol on the dimer stability. Particularly, the results of GXXXG1 and GXXXG2 clarify distinct and strong constraints by membrane

cholesterol on the stability of TM helix dimers. Consistent with the existing literature,[2b, 2c] we confirmed that steric hindrance and packing around the Gly-containing interface determined packed dimer structures (crossing angles of ~10° for GXXXG1 (categorized to left-handed parallel association) and ~55° for GXXXG2 (categorized to right-handed parallel association). In addition, we observed that multiple Gly residues tend to inhibit the formation of stable dimers due to the large flexibility of helix main chains (e.g., GXXXG3). Importantly, our results strongly support a hypothetical mechanism in which membrane environment is critical to stabilizing the candidate packed dimers, i.e., helix dimers with small (<10°, GXXXG1) and large (~55°, GXXXG2) crossing angles were only stabilized in POPC and POPC/cholesterol membranes, respectively. The present results are consistent with the following view that 1) amino acid sequences dictate potential packed dimer structures with different crossing angles, while 2) the properties of lipid membranes, such as a higher lateral pressure in the hydrocarbon core induced by cholesterol, dominantly constraints the stability of helix dimers. Considering that the plasma membranes of animal cells contain significant amounts of cholesterol (25–50% of total lipids),[5e] this

can be relevant to biological/physiological systems. For example, the TM region of neuropilin-1 receptor, which mediates signaling in the development of nervous and vascular systems, has a GXXXGXXXG sequence, which is essential for dimerization and signaling in response to class 3 semaphorin ligands.[17] Recent studies also suggest that neuropilin-1 is a co-receptor of SARS-CoV-2 infection.[18] Neuropilin-1 is a cholesterol-dependent receptor, and is proposed to be recruited to the raft domain (enriched in cholesterol and sphingolipids) upon binding of the ligands, however, the recruitment mechanism is not known.[19] Our hypothetical model may be a compelling explanation of this recruitment behavior, e.g., the ligand binding stabilizes the GXXXGXXXG-mediated X-shaped dimer of neuropilin-1 and the dimer formation enhances partitioning to the cholesterol-rich raft domain via preferential interactions between X-shaped dimer and cholesterol-rich membranes, although it is important to demonstrate the stabilization of X-shaped dimer of neuropilin-1 TM domain in the presence of cholesterol. This might be tested using corresponding TM peptides, although more complex interactions are potentially involved in the natural sequence. As described in this implication, the elaborate interplay between amino acid sequences and

lipid compositions may be a regulatory mechanism of membrane protein functions in biological membranes, although the further range of TM peptides, including those from real proteins, should be analyzed to increase the generality of the conclusion in future research.

## Experimental Section

**Peptide Synthesis.**

Chromophore-labeled transmembrane peptides were manually synthesized using the standard 9-fluorenylmethoxycarbonyl (Fmoc)-based method on NovaSynTGR resin (Millipore, Billerica, MA, USA). Fmoc-amino acids were coupled for 2 h on the resin with 3 eq. amounts of amino acids, HOBt, and *N*,*N*'-diisopropylcarbodiimide in *N*,*N*-dimethylformamide (DMF). The reaction was monitored using the ninhydrin test. Fmoc was removed by treatment with 20% piperidine in DMF for 20 min. Chromophores (Cy3B, Cy5, and NBD) were labeled at the N terminus of the peptides on resin by treatment with succinimidyl esters (Cy3B and Cy5) (GE Healthcare, Little Chalfont, United Kingdom) or the chloride derivative (NBD) (Nacalai Tesque, Kyoto,

Japan) in DMF containing 5% *N,N*-diisopropylethylamine for 48 h. The peptide was cleaved from the resin with a deprotection cocktail of TFA/thioanisole/*m*-cresol/ethanedithiol/$H_2O$ (16/1/1/1/1, v/v). Regarding the formation of heterodimers, the cysteine thiols of Cy3B-labeled peptides were activated by the addition of 800 mM 2,2'-dithiodipyridine in the deprotection step (TFA/thioanisole/*m*-cresol/triisopropylsilane/$H_2O$ (32/2/2/1/2, v/v)).[20] The parallel dimer was synthesized by the formation of disulfide bonds between Cy3B-β-C-β-GXXXG and Cy5-β-C-β-GXXXG (β indicates β-alanine) in DMSO/acetic acid/$H_2O$ (95/2/3, v/v) at 40°C for 6 days. Disulfide-bridged dimer peptides except GXXXG3 were purified by a PLRP-S 300 Å 5-μm reversed-phase HPLC column (Agilent, Santa Clara, CA, USA) with a linear gradient from formic acid/$H_2O$ (2/3, v/v) to formic acid/2-propanol (4/1, v/v) at 50°C. GXXXG3 was purified by the PLRP-S column with a linear gradient from water/0.1% TFA to acetonitrile/0.1% TFA at 40°C. The eluted peptide solution was immediately evaporated with a water bath (70°C) and lyophilized. The peptide powder was dissolved in 1,1,1,3,3,3-hexafluoroisopropanol and identified by matrix-assisted laser desorption/ionization mass spectroscopy. The purities of the disulfide-bridged

peptides were >88% (HPLC).

**Single-Pair FRET.**

Measurements and data analyses were performed as described in a previous study[9b] unless otherwise noted. The biotin-PEG-coated slide chamber for fixing large unilamellar vesicles (LUVs) was prepared based on the protocol of Joo and Ha.[21] Briefly, a No. 1-S cover glass (24 × 60 mm, Matsunami Glass, Osaka, Japan) was washed by sonication in 1 M KOH and methanol, amino-functionalized with aminopropylsilane, and then coated with biotinylated PEG by treatment with PEG succinimidyl ester, with an average MW of 5,000 (mPEG-SVA, Laysan Bio, Arab, AL, USA), and its biotin derivative (biotin-PEG-SVA, Laysan Bio) at a ratio of 80/1 (w/w). A quartz slide (26 × 76 × 1 mm) with inlet/outlet holes (diameter of 1 mm) and an outlet tube was custom-made by DAICO MFG (Kyoto, Japan). The chamber was assembled by placing a silicon spacer (thickness of 0.2 mm) between the cover glass and slide to form a chamber space of ~60 μL. Samples were introduced into the chamber by suctioning a droplet on the inlet hole from the outlet side with a syringe pump (Nanojet,

Chemix, Stafford, TX, USA).

The lipids 1-palmitoyl-2-oleoyl-*sn*-glycero-3-phosphatidylcholine (POPC), 1,2-dipalmitoyl-*sn*-glycero-3-phosphoethanolamine-N-(cap biotinyl) (biotin-PE), and cholesterol were obtained from Avanti Polar Lipids (Alabaster, AL, USA). Disulfide dimer peptides were incorporated into membrane films by mixing with lipids in organic solvents. POPC/cholesterol/biotin-PE/peptide (630,000/270,000/9,000/1) or POPC/biotin-PE/peptide (900,000/9,000/1) was dissolved in ethanol or 2,2,2-trifluoroethanol, respectively, followed by evaporation. The membrane film was dried under a vacuum pump overnight. The film was hydrated with fresh Tris buffer (10 mM Tris/150 mM NaCl/1 mM EDTA supplemented with 0.8% (w/v) D-glucose and 1 mM Trolox (pH 7.4)) at 50°C for 20–30 min to obtain multilamellar vesicles (total lipid concentration of 5–15 mM). LUVs were prepared by extrusion of the membrane suspension through a polycarbonate filter with 100-nm pores (31 times) at 50°C.

Biotinylated LUVs (~ 1:100 dilution) were added to the biotin-PEG-coated chamber and incubated for 10 min following a 10-min pretreatment with 0.2 mg $mL^{-1}$

NeutrAvidin. After fixing, LUVs were incubated with 100 mM 2-mercaptoethanol for 30 min to cleave disulfide bonds.

Fluorescence images for Cy3B (575−635 nm) and Cy5 (645−745 nm) under Cy3B excitation at 561 nm were simultaneously acquired using a Nikon Ti-based total internal reflection microscope equipped with an ImagEM EM-CCD camera and W-View optics (Hamamatsu Photonics, Hamamatsu, Japan) at a time resolution of 17 ms. To suppress photoblinking, observations were performed in oxygen-depleted Tris buffer containing 1 mM Trolox, 1 mM methyl viologen, 0.8% (w/v) D-glucose, 0.25 mg $mL^{-1}$ glucose oxidase, and 10.5 mg $mL^{-1}$ catalase (pH 7.4). After measurements, the number of helices was measured by stepwise photobleaching. We selected vesicles that had incorporated only one donor helix and one acceptor helix for the FRET analysis. The apparent FRET efficiency, $E_{app}$, was calculated from fluorescence intensities for the donor ($F_{Cy3B}$) and acceptor ($F_{Cy5}$) as $E_{app} = F_{Cy5} / (F_{Cy3B} + F_{Cy5})$. sp-FRET trajectories originating from monomer−dimer transitions were analyzed with the HaMMy program (http://bio.physics.illinois.edu/HaMMy.asp) to deduce rate constants between different states. Assuming two-state dynamics, the rate constants for dimer formation ($k_{on}$) and

dimer dissociation ($k_{off}$) were obtained from the transition probabilities (*tp*) as *k* = (*tp*)*(data acquisition rate (Hz)). The fraction of associated helices ($f_a$) was estimated from rate constants as follows:

$$f_a = \frac{k_{on}}{k_{on}+k_{off}} \quad (1)$$

The association constant ($K_a$) and corresponding Gibbs free-energy change ($\Delta G_a$) are given by

$$\Delta G_a = -RTlnK_a \quad (2)$$

$$K_a = \frac{[D]}{[M]^2} \quad (3)$$

*R* and *T* represent the gas constant and absolute temperature, respectively. [M] and [D] denote the mole fraction of the helix monomer and dimer, respectively, in the bilayers, which are related to $f_a$ as

$$[\mathrm{M}] = (1 - f_a)\frac{2n_p}{2n_p+n_l} \qquad (4)$$

$$[\mathrm{D}] = \frac{2f_a n_p}{2(2n_p+n_l)} = \frac{f_a n_p}{2n_p+n_l} \qquad (5)$$

with the number of peptides (= 2) and lipids (= 90,000) in a vesicle being denoted by $n_p$ and $n_l$, respectively. A factor of 2 was introduced to take the TM nature of the peptide into consideration.[9d]

**Prediction of Dimer Structures with PREDDIMER.**

3D models of helix dimers were constructed using the PREDDIMER web server.[12a] The amino acid sequences of GXXXG helices were entered to search for packed homodimer structures. The structure with the best packing score ($F_{scor}$) was used as a dimer model.

**FTIR-PATR.**

NBD-labeled peptides were used for IR measurements. The oriented films of lipids/peptides were prepared by uniformly spreading 100 μL of an ethanol solution of

lipids (5 μmol) and peptides (5 nmol) on a germanium ATR plate (70 × 10 × 5 mm), followed by evaporation of the solvent with $N_2$ gas under a vacuum overnight. Films were hydrated with a $D_2O$-soaked piece of filter paper placed over the plate at 25°C for 3 h. Fourier transform infrared-polarized attenuated total reflection (FTIR-PATR) measurements were conducted as previously described[9a] on a Bruker TENSOR27 spectrometer equipped with a Specac horizontal ATR attachment with an AgBr polarizer and temperature controller. The dichroic ratio, *R*, defined by $\Delta A_{/\!/}/\Delta A_{\perp}$, was calculated from polarized spectra. Absorbance ($\Delta A$) was obtained as the area for the amide I' band. Subscripts $/\!/$ and $\perp$ refer to polarized light with the electric vector parallel and perpendicular, respectively, to the plane of incidence. The average helix orientation angle (defined as the angle between the helix axis and the normal direction of the membrane plane), $\alpha$, was calculated from *R*.

$$cos^2 a = \frac{1}{3}\left(\frac{4}{3cos^2\theta - 1} \cdot \frac{R - 2.00}{R + 1.45} + 1\right) \qquad (6)$$

We assumed a fixed angle ($\theta$) of 35° between the helix axis and transition moments for amide I' bands. The crossing angle of the hypothetical helix dimer (defined as the angle between the axes of the helices) shown in Table 2 was estimated to be double the orientation angle ($2\alpha$), assuming 1) all peptides assume helix dimers and 2) a two-fold axial symmetry of the dimer to the bilayer normal direction.

## Acknowledgments

We thank Prof. Masaru Hoshino (Kyoto University) for his technical advice about the formation of dimer peptides. This work was supported by a JSPS KAKENHI Grant-in-Aid for Scientific Research (C) (19K07013) (Y.Y.).

## Keywords:

single-molecule studies • membrane proteins • GXXXG • lipids • cholesterol

# References


[1] a) D. M. Engelman, Y. Chen, C. N. Chin, A. R. Curran, A. M. Dixon, A. D. Dupuy, A. S. Lee, U. Lehnert, E. E. Matthews, Y. K. Reshetnyak, A. Senes, J. L. Popot, *FEBS Lett.* **2003**, *555*, 122–125; b) S. H. White, W. C. Wimley, *Annu. Rev. Biophys. Biomol. Struct.* **1999**, *28*, 319–365.

[2] a) W. P. Russ, D. M. Engelman, *J. Mol. Biol.* **2000**, *296*, 911–919; b) R. F. Walters, W. F. DeGrado, *Proc. Natl. Acad. Sci. U.S.A.* **2006**, *103*, 13658–13663; c) S. Q. Zhang, D. W. Kulp, C. A. Schramm, M. Mravic, I. Samish, W. F. DeGrado, *Structure* **2015**, *23*, 527–541.

[3] a) E. Li, W. C. Wimley, K. Hristova, *Biochim. Biophys. Acta* **2012**, *1818*, 183-193; b) M. G. Teese, D. Langosch, *Biochemistry* **2015**, *54*, 5125–5135.

[4] A. G. Lee, *Biochim. Biophys. Acta* **2004**, *1666*, 62–87.

[5] a) J. Fantini, F. J. Barrantes, *Front. Physiol.* **2013**, *4*, 31; b) M. A. Hanson, V. Cherezov, M. T. Griffith, C. B. Roth, V. P. Jaakola, E. Y. Chien, J. Velasquez, P. Kuhn, R. C. Stevens, *Structure* **2008**, *16*, 897–905; c) M. Manna, M. Niemela, J. Tynkkynen, M. Javanainen, W. Kulig, D. J. Muller, T. Rog, I. Vattulainen, *Elife*

**2016**, *5*, e18432; d) A. B. Pawar, D. Sengupta, *J. Membr. Biol.* **2021**, *254*, 301–310; e) Y. Song, E. J. Hustedt, S. Brandon, C. R. Sanders, *Biochemistry* **2013**, *52*, 5051–5064.

[6] a) V. Anbazhagan, D. Schneider, *Biochim. Biophys. Acta* **2010**, *1798*, 1899–1907; b) R. S. Cantor, *Biophys. J.* **2002**, *82*, 2520–2525; c) E. van den Brink-van der Laan, J. A. Killian, B. de Kruijff, *Biochim. Biophys. Acta* **2004**, *1666*, 275–288.

[7] a) F. Cornelius, *Biochemistry* **2001**, *40*, 8842–8851; b) G. Gimpl, K. Burger, F. Fahrenholz, *Biochemistry* **1997**, *36*, 10959–10974; c) L. Pang, M. Graziano, S. Wang, *Biochemistry* **1999**, *38*, 12003–12011.

[8] a) C. Choma, H. Gratkowski, J. D. Lear, W. F. DeGrado, *Nat. Struct. Biol.* **2000**, *7*, 161–166; b) S. Mall, R. Broadbridge, R. P. Sharma, J. M. East, A. G. Lee, *Biochemistry* **2001**, *40*, 12379–12386; c) E. Sparr, W. L. Ash, P. V. Nazarov, D. T. Rijkers, M. A. Hemminga, D. P. Tieleman, J. A. Killian, *J. Biol. Chem.* **2005**, *280*, 39324–39331.

[9] a) Y. Yano, K. Kondo, R. Kitani, A. Yamamoto, K. Matsuzaki, *Biochemistry*

**2015**, *54*, 1371–1379; b) Y. Yano, K. Kondo, Y. Watanabe, T. O. Zhang, J. J. Ho, S. Oishi, N. Fujii, M. T. Zanni, K. Matsuzaki, *Angew. Chem. Int. Ed. Engl.* **2017**, *56*, 1756–1759; c) Y. Yano, K. Matsuzaki, *Biochemistry* **2006**, *45*, 3370–3378; d) Y. Yano, T. Takemoto, S. Kobayashi, H. Yasui, H. Sakurai, W. Ohashi, M. Niwa, S. Futaki, Y. Sugiura, K. Matsuzaki, *Biochemistry* **2002**, *41*, 3073–3080; e) Y. Yano, Y. Watanabe, K. Matsuzaki, *Biochim. Biophys. Acta Biomembr.* **2021**, *1863*, 183532; f) Y. Yano, A. Yamamoto, M. Ogura, K. Matsuzaki, *Biochemistry* **2011**, *50*, 6806–6814.

[10] I. V. Korendovych, W. F. DeGrado, *Q. Rev. Biophys.* **2020**, *53*, e3.

[11] a) N. Castillo, L. Monticelli, J. Barnoud, D. P. Tieleman, *Chem. Phys. Lipids* **2013**, *169*, 95–105; b) H. Itaya, K. Kasahara, Q. Xie, Y. Yano, K. Matsuzaki, T. Takahashi, *ACS Omega* **2021**, *6*, 11458–11465; c) A. B. Pawar, S. A. Deshpande, S. M. Gopal, T. A. Wassenaar, C. A. Athale, D. Sengupta, *Phys. Chem. Chem. Phys.* **2015**, *17*, 1390–1398.

[12] a) P. Anton, "PREDDIMER", can be found under http://preddimer.nmr.ru, **2013**; b) A. A. Polyansky, A. O. Chugunov, P. E. Volynsky, N. A. Krylov, D. E. Nolde,

R. G. Efremov, *Bioinformatics* **2014**, *30*, 889–890.

[13] Y. Yano, *Chem. Pharm. Bull. (Tokyo)* **2022**, *70*, 514-518.

[14] R. S. Cantor, *Biophys. J.* **1999**, *76*, 2625–2639.

[15] P. Hogel, A. Gotz, F. Kuhne, M. Ebert, W. Stelzer, K. D. Rand, C. Scharnagl, D. Langosch, *Biochemistry* **2018**, *57*, 1326–1337.

[16] R. M. Johnson, A. Rath, C. M. Deber, *Biochem. Cell. Biol.* **2006**, *84*, 1006–1012.

[17] L. Roth, C. Nasarre, S. Dirrig-Grosch, D. Aunis, G. Cremel, P. Hubert, D. Bagnard, *Mol Biol, Cell.* **2008**, *19*, 646–654.

[18] R. Rangu, P. L. Wander, B. M. Barrow, S. Zraika, *J. Mol. Endocrinol.* **2022**, *69*, R63–R79.

[19] A. Salikhova, L. Wang, A. A. Lanahan, M. Liu, M. Simons, W. P. Leenders, D. Mukhopadhyay, A. Horowitz, *Circ. Res.* **2008**, *103*, e71–79.

[20] C. M. Yamazaki, S. Asada, K. Kitagawa, T. Koide, *Biopolymers* **2008**, *90*, 816–823.

[21] C. Joo, T. Ha, *Cold Spring Harb. Protoc.* **2012**, *2012*, 1104–1108.

**Table 1**: Amino acid sequences of GXXXG-introduced model transmembrane helices.

Substituted residues and Gly-containing motifs are shaded and underlined, respectively.

| Name | Sequence |
|---|---|
| Host | AALALAA AALALAA AALALAA |
| GXXXG1 | AALALAA AGLALGA AALALAA |
| GXXXG2 | AALALAA AGLALGA AAGALAA |
| GXXXG3 | AALALGA AGLALGA AGAALAA |
| GXXXG4 | AALAALA AGLALGA ALAALAA |
| GXXXG5 | AGLALGA AALALAA AALALAA |

**Table 2**: Summary of crossing angles predicted by PREDDIMER and estimated by FTIR-PATR measurements ($n$ = 3).

| | PREDDIMER | FTIR-PATR | |
|---|---|---|---|
| | | POPC | POPC/cholesterol (7/3) |
| GXXXG1 | 10.4° | ~20° | ~20° |
| GXXXG2 | 55° | ~12° | ~52° |

# Table of contents

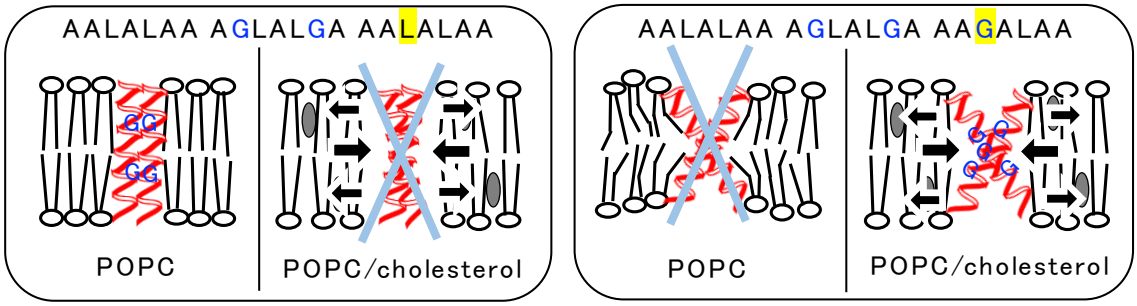


Small residue-mediated interhelical packing is ubiquitous in helical membrane proteins; however, the lipid dependence of its stability remains unclear. A single-molecule study of *de novo*-designed transmembrane helices revealed elaborate regulation by cholesterol. A change of only single amino acid (L17G) completely reversed the cholesterol dependence of helix dimerization.

*Supporting Information*

# Effects of Gly residue and Cholesterol on the GXXXG-Mediated Parallel Association of Transmembrane Helices: A Single-Pair FRET Study

Yoshiaki Yano,[a] Takayuki Morise,[b] and Katsumi Matsuzaki*[b]

[a] Prof. Y. Yano

School of Pharmacy and Pharmaceutical Sciences, Mukogawa Woman's University,

Nishinomiya 663-8179, Japan

[b] T. Morise, Prof. K. Matsuzaki

Graduate School of Pharmaceutical Sciences, Kyoto University, Kyoto 606-8501, Japan

E-mail: mkatsumi@pharm.kyoto-u.ac.jp

**Supporting Figures**

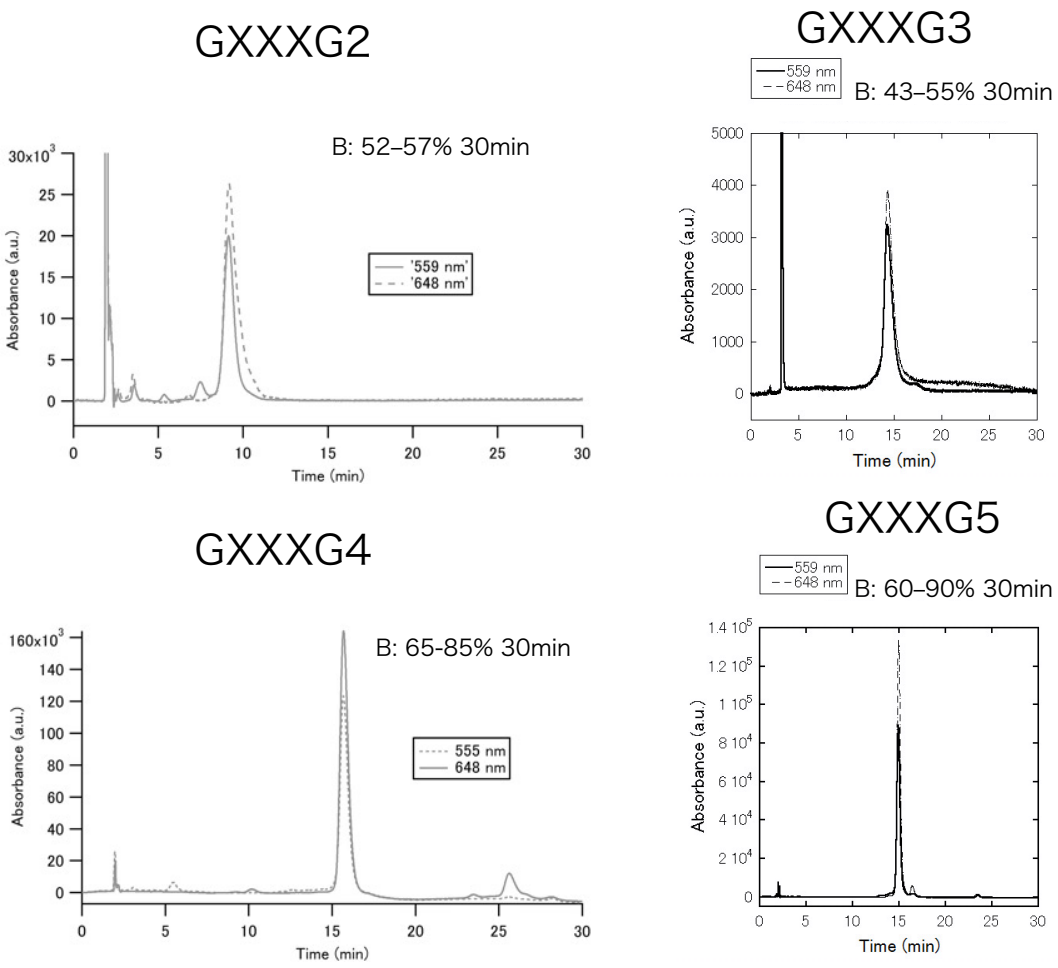


Supporting Figure S1

HPLC chromatograms of synthetic crosslinked dimer peptides.

Disulfide-bridged dimer peptides were purified by a PLRP-S column with a linear gradient from (A) formic acid/$H_2O$ (2/3, v/v) to (B) formic acid/2-propanol (4/1, v/v) at 50°C. GXXXG3 was purified by the PLRP-S column with a linear gradient from (A) water/0.1% TFA to (B) acetonitrile/0.1% TFA at 40°C. The percentage of (B) in the gradient was shown in the figure.

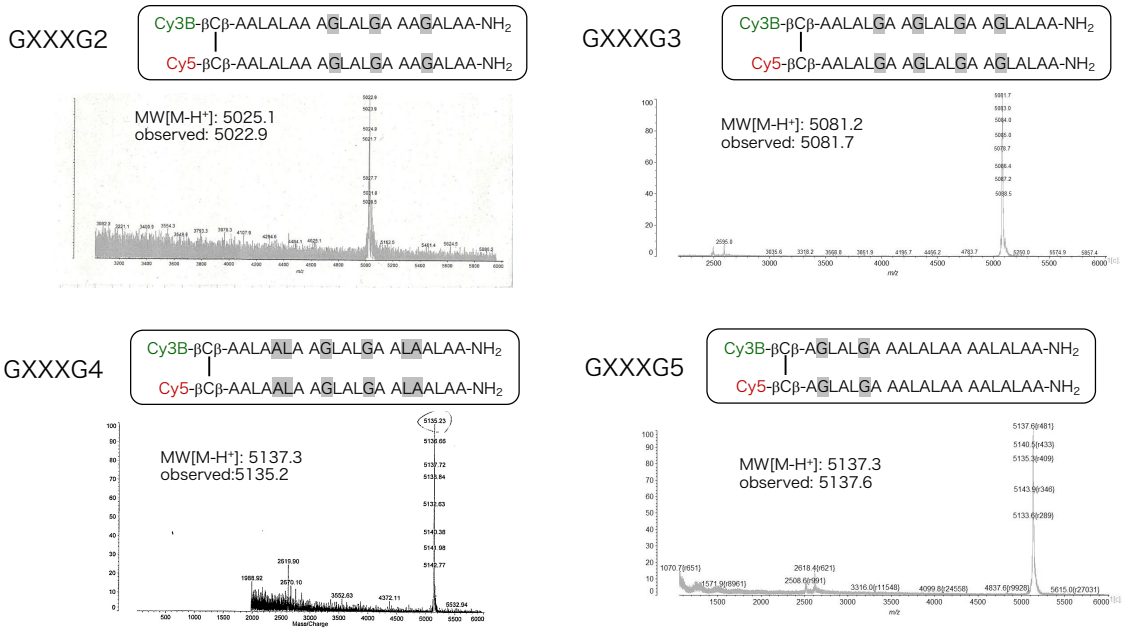


Supporting Figure S2

Mass chromatograms of synthetic crosslinked dimer peptides.

Theoretical and observed molecular weights are shown in the figure.

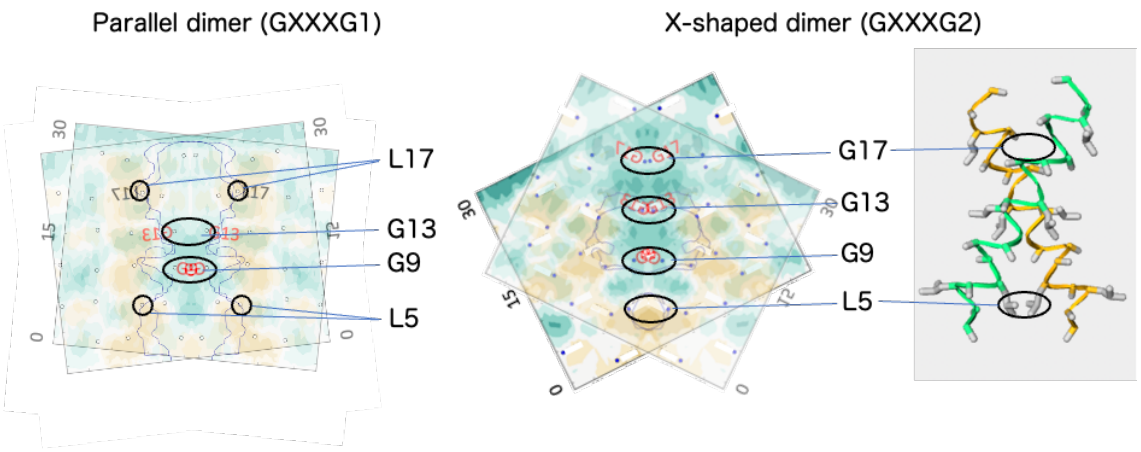


Supporting Figure S3

To visualize the positions of residues 5, 9, 13, and 17 in the parallel (left) and X-shaped (right) dimers, two surface maps of PREDDIMER were overlapped (one map was inverted). These four residues are along with the center line of the interface in the X-shaped dimer, whereas the positions 5 and 17 are adjacent to the interface in the parallel dimer. In the X-shaped dimer, the helix main chains at the positions 5 and 17 fall outside of the interface due to the helix tilt (see green and yellow chains in 3D image in the right figure generated with GLmol), however, the side chains (gray) of these positions can sterically interfere with each other. In the case of GXXXG2, the side chain packing of L5 forms a part of the helix–helix interface, whereas the L17G substitution is expected to reduce steric hindrance at the position.

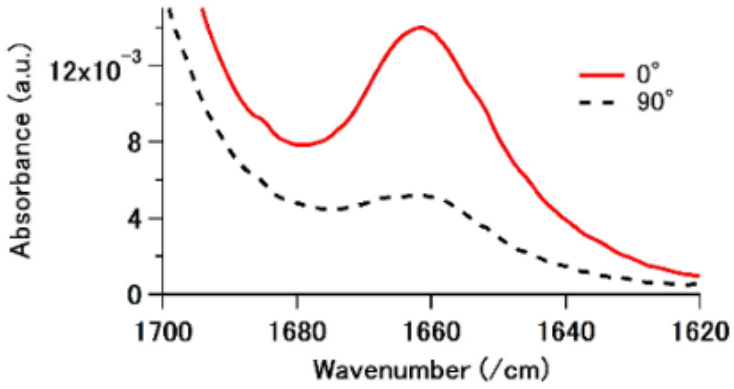


Supporting Figure S4

FTIR-PATR spectra. (a) FTIR-PATR spectra of NBD-GXXXG2 (amide I' region). Solid and dotted lines indicate the spectra for polarized light with its electric vector parallel (0°) and perpendicular (90°) to the plane of incidence, respectively.

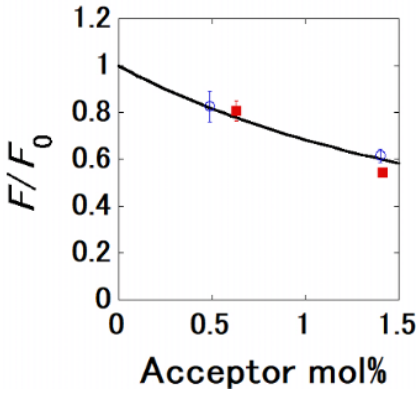


Supporting Figure S5

Fluorescence quenching of dehydroergosterol with N-(7-nitrobenz-2-oxa-1,3-diazol-4-yl)-1,2-dihexadecanoyl-sn-glycero-3-phosphoethanolamine (NBD-PE, red squares) and NBD-labeled GXXXG2 (blue circles). The molar ratio of POPC/cholesterol/dehydroergosterol was fixed at 70/29/1. The fluorescence intensity from dehydroergosterol (excitation: 300 nm; emission: 374 nm) was measured in the presence of acceptor NBD molecules. The gray line indicates a theoretical quenching curve expected for random FRET assuming an $R_0$ of 30 Å and the distance of the closest approach (Rc) of 25.8 Å. [1, 2]

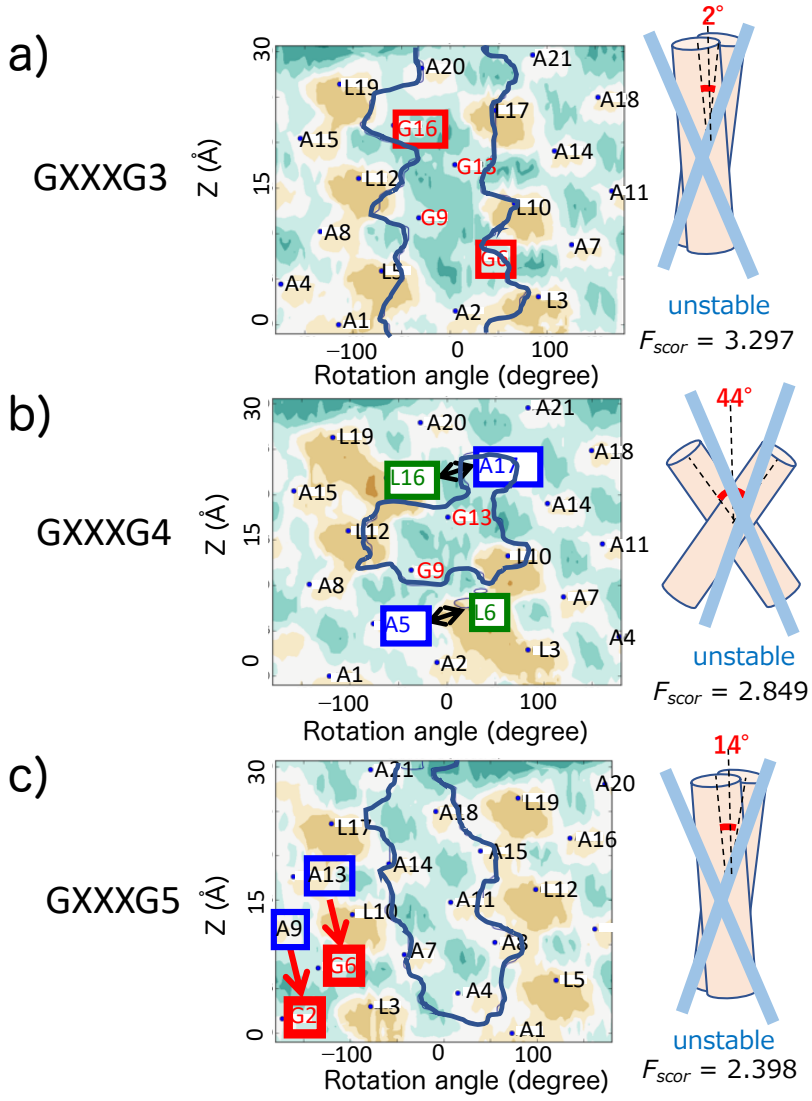


Supporting Figure S6

Helix interaction interface of best-scoring dimers by PREDDIMER for GXXXG3 (a), GXXXG4 (b), and GXXXG5 (c). Horizontal and vertical axes indicate the helix rotation angle and distance along the helix (0 Å at the N terminus of the helix), respectively. Green and sand colors indicate concave and convex on the surface, respectively. The association interface region was surrounded by blue lines. Substituted or exchanged residues were marked with rectangles and colored with red (Gly), blue (Ala), and green (Leu). The right image shows the shapes of dimers.

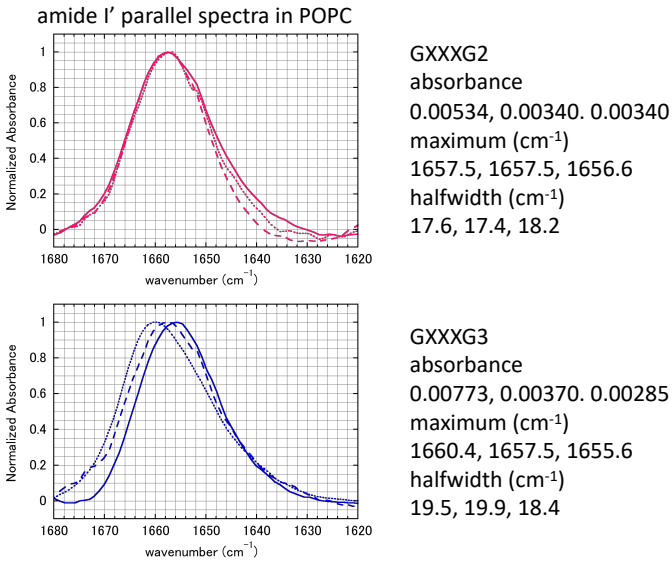


Supporting Figure S7

PATR-FTIR parallel amide I ' spectra of GXXXG2 (upper) and GXXXG3 (lower) in POPC membranes. Three spectra were shown for each peptide. The lipid background was subtracted to compare the linewidths of spectra. The values of absorbance, the wavenumbers of maximal absorption, and the full width at half-maximal (halfwidth) were described in the figure.

Supporting References

[1] Y. Yano, K. Kondo, R. Kitani, A. Yamamoto, K. Matsuzaki, Cholesterol-induced lipophobic interaction between transmembrane helices using ensemble and single-molecule fluorescence resonance energy transfer, Biochemistry **2015**, *54*, 1371.
[2] P. K. Wolber, B. S. Hudson, An analytic solution to the Förster energy transfer problem in two dimensions, Biophys. J. **1979**, *28*, 197.